

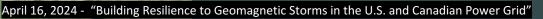


### Adam Schultz

National Geoelectromagnetic Facility

College of Earth, Ocean and Atmospheric Sciences

**Oregon State University** 



## Evolution of the MTArray – Magnetotelluric measurements used to mitigate risk to the power grid from space weather

For the past 18-years Oregon State University and its contractors - under the support of NSF (2006-2018), NASA (2019-2020) and USGS (2020-2024)- installed temporary (weeks-to-months; at 7 Backbone stations - years) long-period MT stations that measure ground-level vector electric and magnetic fields on a 70-km grid of points spanning the conterminous US.

A total of 1711 transportable stations whose data meet data quality control standards will have been installed, operated and extracted by mid-2024, completing the MTArray in CONUS.

We generate MT Impedance tensors ("EMTF"s, induction vectors and related quantities from the MT time series, suitable for determining the 3-D electrical structure of the crust and upper mantle.

The impedances, induction vectors, and/or derived 3-D electrical models can be used to estimate ground-level electric fields from measurements or models of ground-level magnetic fields. These can be integrated along the paths of power grid transmission lines and flowed through power grid equivalent electrical circuits to determine GIC intensity, transformer heat and vibration, and reactive power loss.

A look to the future: With a sufficiently dense, real-time telemetering network of MT stations, we have demonstrated how a convolutional neural network trained on measured time series from an array of MT stations may be used to forecast ground-level fields more than 30-minutes in the future, and the potential this has for alerting power utilities of incoming risks to specific HV transformers on the transmission network (reported at this workshop in 2022).

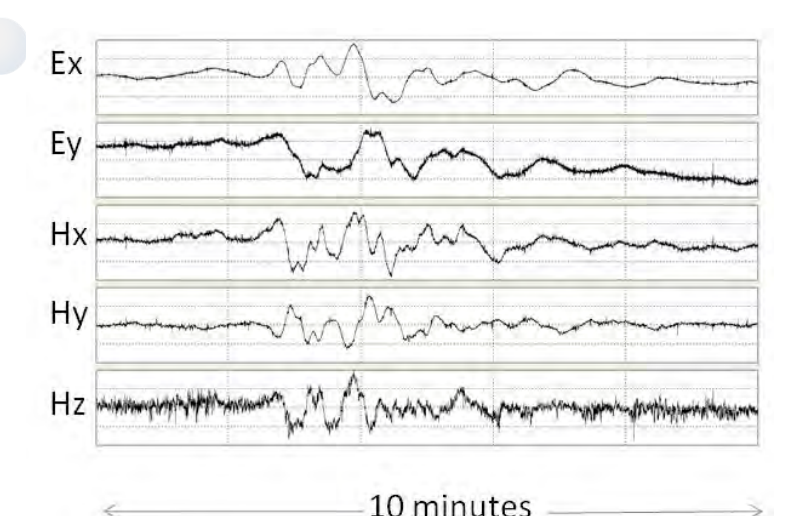
## The Magnetotelluric Method (MT)

We measure two orthogonal horizontal electric field components  $E_x(t)$  and  $E_y(t)$ , and three orthogonal magnetic field components  $H_x(t)$ ,  $H_y(t)$ ,  $H_z(t)$ .

After sophisticated signal analysis, these are transformed into corresponding electric and magnetic frequency spectra, i.e.  $E_x(t) \iff \tilde{E}_x(f)$ 

We then form estimates of the MT *Impedance tensor* (or "EMTF") **Z**, a complex-valued 4 x 4 tensor defined at a set of discrete frequencies – each representing a different depth of penetration sampling a different volume average of the subsurface.

We also form estimates of the MT *Induction vector* (or "Tipper") T, the ratio of vertical to horizontal magnetic field components.



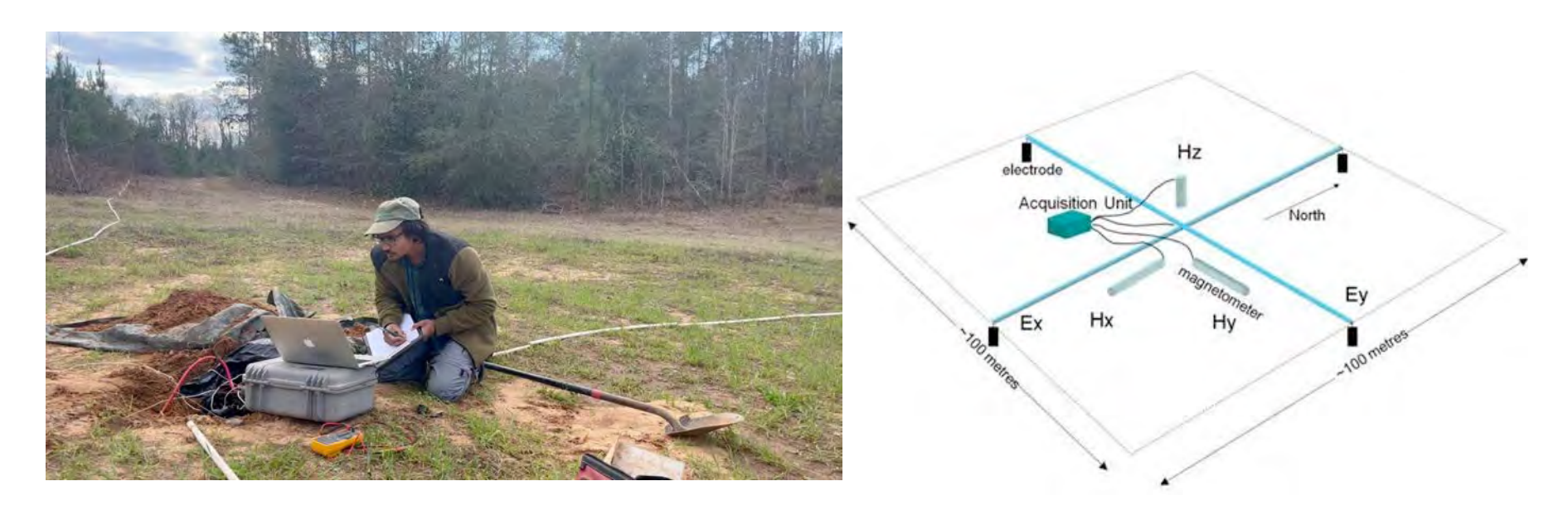
$$\begin{bmatrix} E_x \\ E_y \end{bmatrix} = \begin{bmatrix} Z_{xx} & Z_{xy} \\ Z_{yx} & Z_{yy} \end{bmatrix} \begin{bmatrix} H_x \\ H_y \end{bmatrix} + U,$$

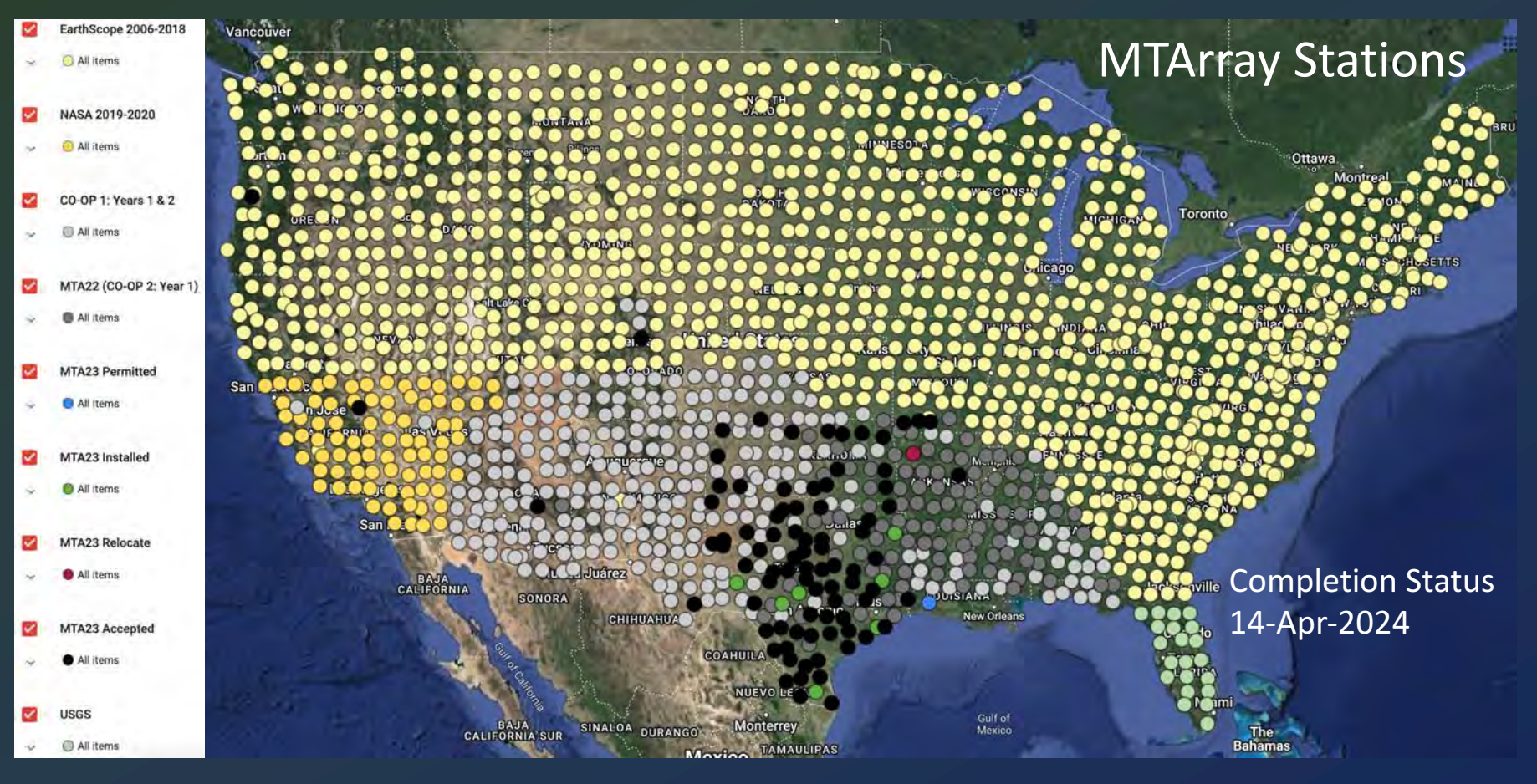
$$H_Z = \begin{bmatrix} H_x & H_y \end{bmatrix} \begin{bmatrix} T_x \\ T_y \end{bmatrix} + U.$$

### The Magnetotelluric Method – MTArray field crew installation

By measuring the vector electric and magnetic fields at the Earth's surface, we determine the frequency dependent *impedance tensor*, which we use to image the electrical conductivity structure of the <u>near-surface</u> through the <u>upper mantle</u>.

(left) installing an MT data acquisition system; (right) the two horizontal electric field dipole sensors and two horizontal and one vertical magnetic field sensor.





Array is 99.94% complete. 7 Backbone stations archived, 1695 out of 1711 Transportable stations archived, 6 currently operating, 1 permitted and 1 remaining to permit (2 station installations remain to complete CONUS. 21 addt'l stations installed directly by USGS assimilated into MTArray

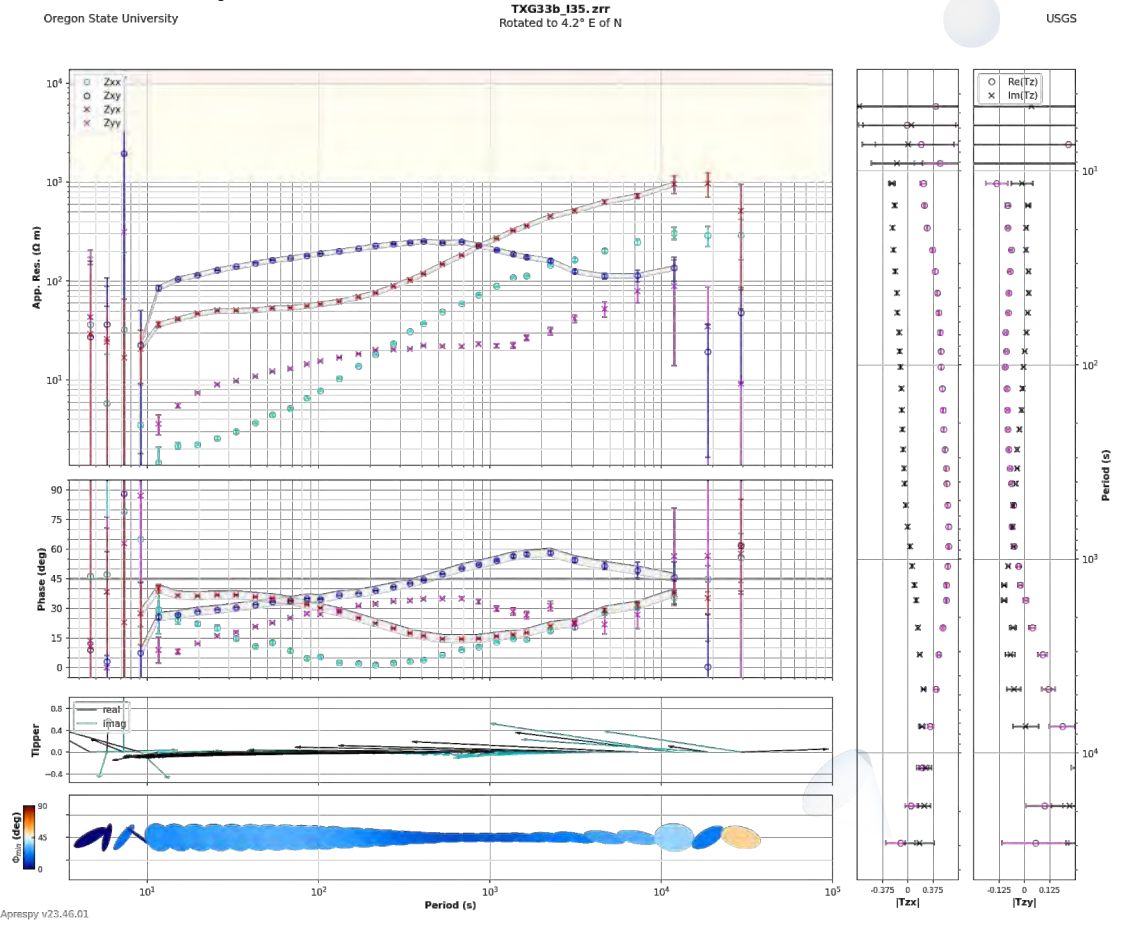
## Magnetotelluric response functions in human-readable form

Each element of the complex-valued impedance tensor can be transformed into real-valued apparent resistivity and phase.  $\rho_a$  is simply the scaled magnitude of the impedance while  $\Phi$  is the phase, i.e. the amount by which the electric field at a given frequency lags or leads the magnetic field in time. If  $\Phi$  > 45° this indicates that the resistivity structure is getting more conductive at whatever depth corresponds to that frequency, and if  $\Phi$  < 45°, more resistive.

$$\rho_{a,xy}(T) = \frac{T}{2\pi\mu_0} \left[ Z_{xy} \right]^2, \qquad \phi_{xy} = \arctan(\frac{Im(Z_{xy})}{Re(Z_{xy})})$$

- If the resistivity varies only with depth (1-D), the relationship between E and H doesn't depend on azimuth, so the impedance tensor reduces to Zxy = -Zyx, Zxx=Zyy=0.
- For 2-D resistivity structure, Zxy and Zyx are defined and their magnitudes are not equal; Zxx=Zyy=0.
- For 3-D resistivity structure, all elements of the impedance tensor are non-zero.

### MT Response Functions



Example of apparent resistivity, phase, tipper and phase tensor data from MTArray station TXG33 near Uvalde, Texas.

The four complex-valued elements of the impedance tensor at each period  $Z_{xx}$ ,  $Z_{xy}$ ,  $Z_{yx}$ , and  $Z_{yy}$  are transformed into the four real-valued elements of apparent resistivity and phase in the top two columns and rows of the figure.

Below this is the real and complex values of the induction vector (Tipper) – the ratio of the vertical magnetic field to the horizontal magnetic field components.

The bottom panel is the phase tensor, revealing the dimensionality of the data and geoelectric strike direction, if defined.

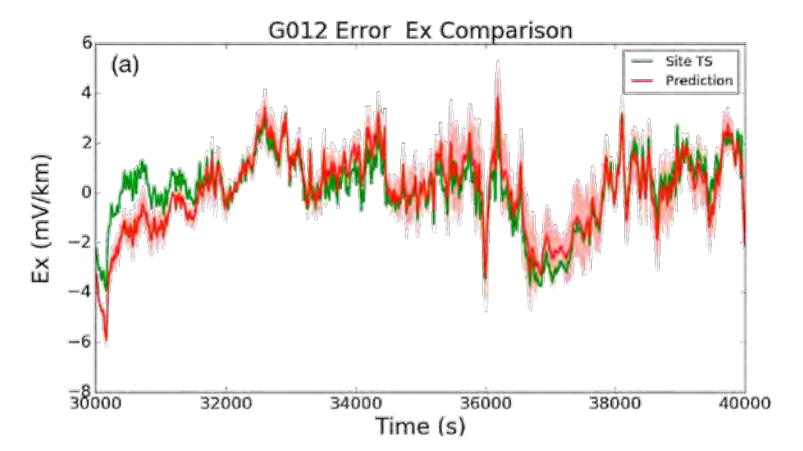
# Predicting ground-level electric fields example from western Oregon

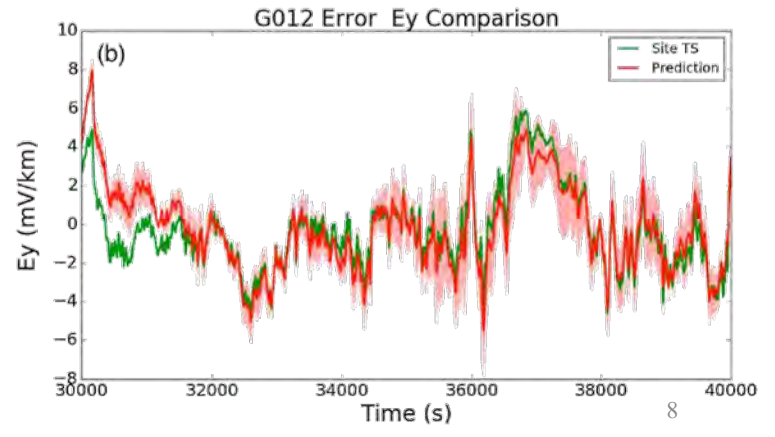
1. Our approach is to pipe the predicted magnetic fields at the locations of former MT stations through the impedance tensors we obtained for those locations, to obtain the predicted electric fields there

$$\begin{bmatrix} \widetilde{E_x} \\ \widetilde{E_y} \end{bmatrix} = \begin{bmatrix} Z_{xx} & Z_{xy} \\ Z_{yx} & Z_{yy} \end{bmatrix} \begin{bmatrix} \widetilde{H_x} \\ \widetilde{H_y} \end{bmatrix} + \begin{bmatrix} \widetilde{U_x} \\ \widetilde{U_y} \end{bmatrix}$$

where the tilde indicates the predicted field.

- 2. We use a distance weighted algorithm to project the predicted electric fields from all the neighboring MT station locations onto each point along the transmission line path.
- 3. Alternatively one can use 3-D models of ground conductivity derived from inversion of the impedance tensors; solve the forward problem, and derive electric fields on a grid of points. This is the USGS/NOAA approach.
- 4. For our approach, electric field prediction misfits at most sites are typically around 1–2 mV/km RMS at the great majority of MT sites that we have examined (for modest  $k_p$  levels, within the BPA operating area) where the distance to the nearest magnetic observatory is < 600 km.





### Wide-scale coherence between E field predicted at Meanook magnetic observatory in Canada and as actually measured by MTArray station TXI36 in Texas

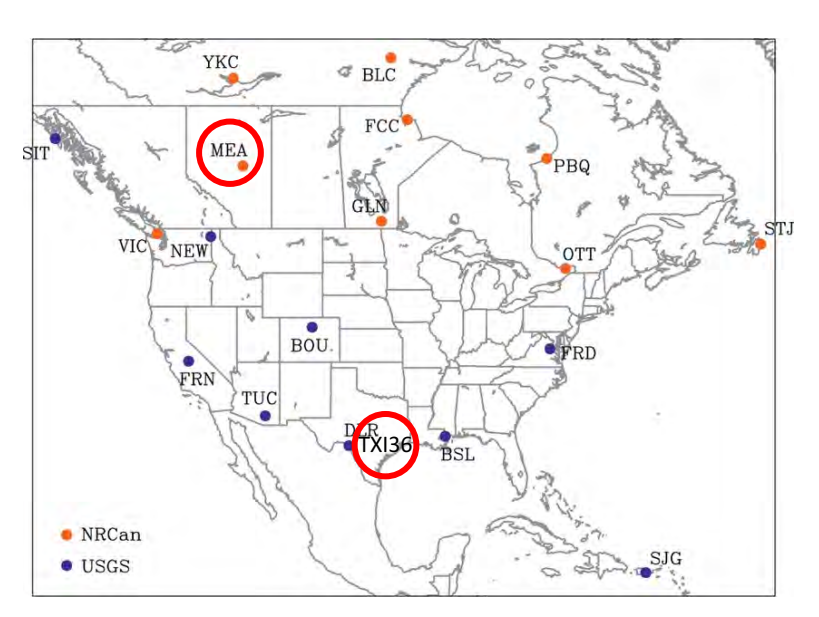
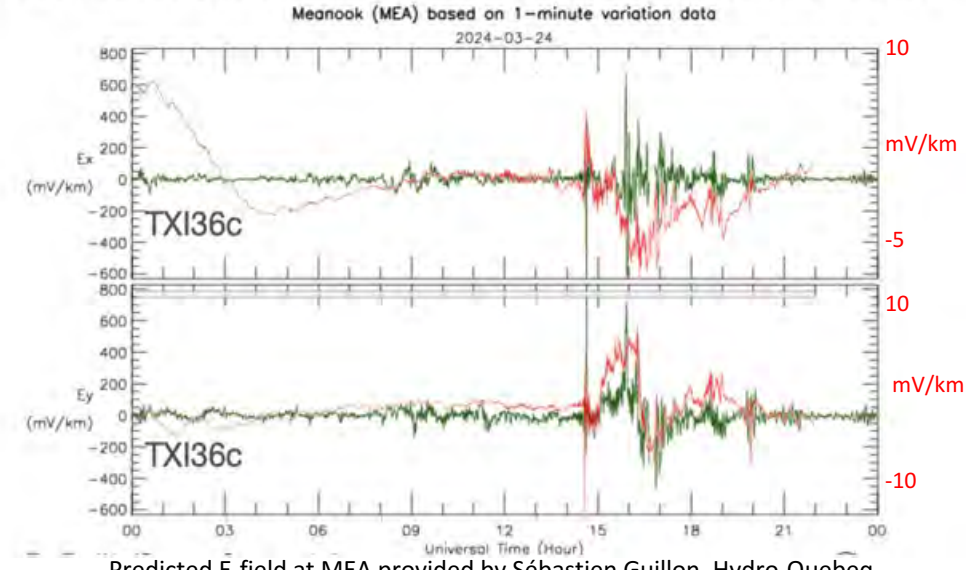


Figure from: Love, Jeffrey et al. (2022). Mapping a Magnetic Superstorm: March 1989 Geoelectric Hazards and Impacts on United States Power Systems. Space Weather. 20. 10.1029/2021SW003030.

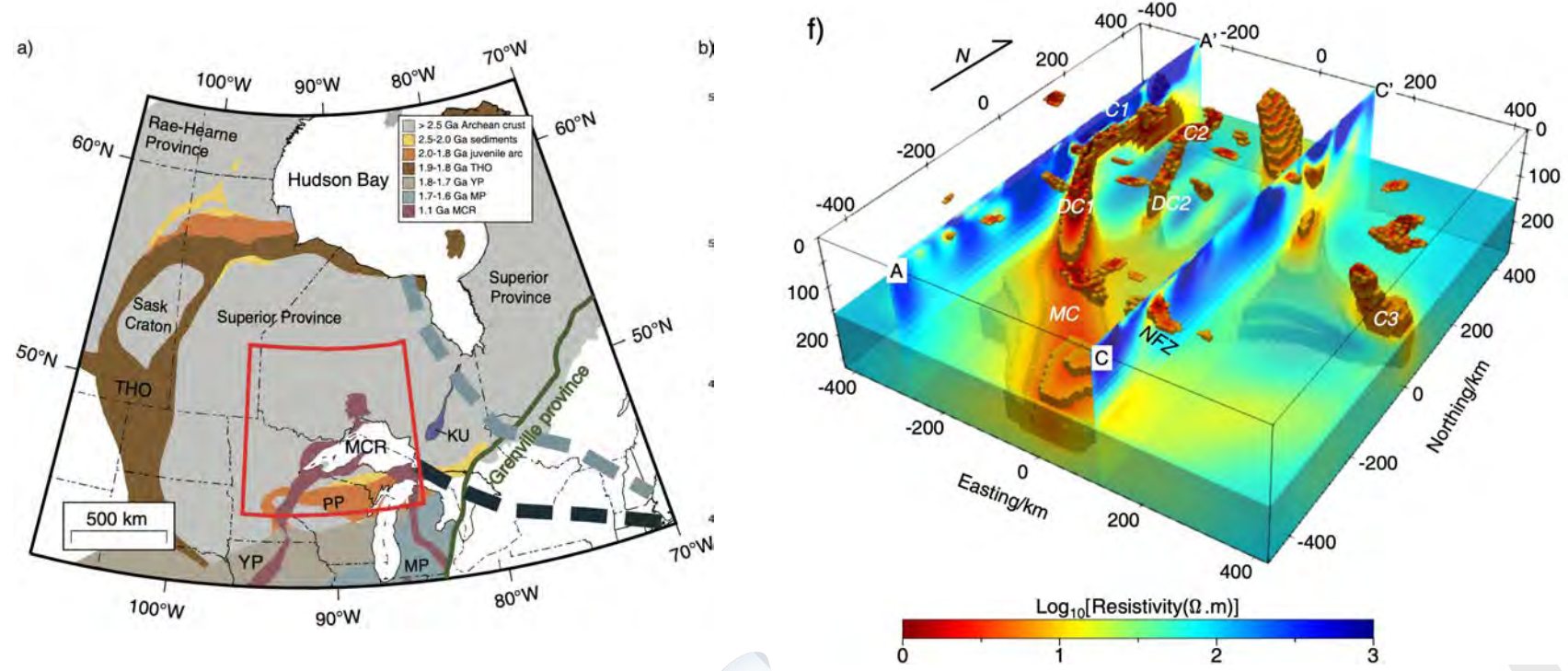
#### NRCan predicted E field at MEA and as measured at US MTArray station TXI36 near Corpus Christi Texas from G4-class GMD on 2024-03-24



Predicted E-field at MEA provided by Sébastien Guillon, Hydro-Quebeg.

The E-field at MEA (green) as predicted by NRCan using regional 1-D conductivity model and actual magnetic fields as measured is nearly 2 orders-of-magnitude greater than E-field as actually measured (red) in highly conductive, nearly 1-D environment near Corpus Christi. This is the exception to the rule – the overwhelming majority of MTArray sites exhibit strong 3-D effects where the E-field magnitude can be amplified by orders-of-magnitude, and where the vector aziumuth and E-field coupling to transmission lines is strongly impacted by 3-D induction effects.

## Mid-Continent Region Example of 3-D Conductivity Structure



a) A simple tectonic map of central North America [18] with the red box showing our study area as shown in b) with more detail. f) A perspective view of high conductivity anomalies (≤ 10 Ω.m) below 20 km depths. Both figures from: Wule, L., A. Schultz, B. Yang and X. Hu. Remnant of 1.1 Ga Midcontinent Rift plume beneath the Superior craton inferred from magnetotelluric data, *National Science Review*, submitted.

### Predicting GICs from MT Impedance and Magnetic Fields at Ground Level

Using measured magnetic fields projected through MT impedance tensors to predict GICs has been validated against measured GICs in power transmission lines, not just in N. America, but globally such as work by:

Marshall, R. A., Wang, L., Paskos, G. A., Olivares-Pulido, G., Van Der Walt, T., Ong, C., et al. (2019). Modeling geomagnetically induced currents in Australian power networks using different conductivity models. Space Weather, **17**, 727–756. https://doi.org/10.1029/2018SW002047

who examined a number of E-field predictions using different regional 1-D and 3-D conductivity models, and concluded that the 3-D approach most closely matched measured GICs in most situations.

Rosenqvist, L., & Hall, J. O. (2019). Regional 3-D modeling and verification of geomagnetically induced currents in Sweden. Space Weather, 17, 27–36. <a href="https://doi.org/10.1029/2018SW002084">https://doi.org/10.1029/2018SW002084</a>

Who developed a 3-D geoelectric model for Fennoscandia and produced an accurate prediction of a measured GIC in Sweden.

Similarly for Spain

Torta, J. M., Marsal, S., Ledo, J., Queralt, P., Canillas-Pérez, V., Piña-Varas, P., et al. (2021). New detailed modeling of GICs in the Spanish power transmission grid. Space Weather, 19, e2021SW002805. <a href="https://doi.org/10.1029/2021SW002805">https://doi.org/10.1029/2021SW002805</a>

etc.

### Archive – how to obtain impedance and other derived MT data

The national archives for long-period MT impedance and related data is at: ds.iris.edu/spud/emtf

Data search can be through the map, or by geographic bounding box, by station name or other designated search fields

